ONLINE FIRST



**ISSN:** 0015-5659

**e-ISSN:** 1644-3284

# Effect of vitamin B17 on experimentally induced colon cancer in adult male albino rat

**Authors**: S. A. Abdel-Rahman, F. E.-N. Abd El-Hady El-Safti, W. Badr El-Kholy, N. Mohey Issa

**DOI:** 10.5603/FM.a2020.0021

**Article type:** ORIGINAL ARTICLES

**Submitted:** 2019-12-13

**Accepted:** 2020-01-23

**Published online:** 2020-02-13

**Effect of vitamin B17 on experimentally induced colon cancer in adult male albino rat**

**Running title:** Effect of vitamin B17 on colon cancer model

S.A. Abdel-Rahman, F. E.-N. Abd El-Hady El-Safti, W. Badr El-Kholy, N. Mohey Issa

Human Anatomy and Embryology, Faculty of Medicine, Menoufia University, Egypt

**Address for correspondence:** S.A. Abdel-Rahman, Assistant lecturer, Human Anatomy and Embryology, Faculty of Medicine, Menoufia University, Egypt (Egypt-Menoufia-Shibin Alkoum-Tiba Tower), e-mail: shireen187@gmail.com

**Abstract**

Colon cancer is considered to be the third most common cancer worldwide. At diagnosis of colon cancer, 3.7-11% developed bone metastasis. Diet based strategies are important for prevention and treatment of colon cancer. This study investigated the effect of vitamin B17 on a DMH induced rat model of colon cancer. Eighty young adult male albino rats were divided into five groups. Group I (control group), Group II (vitamin B17), Group III (CC), Group IV (protected) and Group V (treated). Distal colon sections were prepared for light and scanning electron microscopic examination. Lumbar vertebrae specimens were prepared for light microscopic study. Morphometric and statistical analysis were done. In comparison with the control, both CC and treated groups showed invasion of the colonic tissue by pleomorphic branching colonic glands of variable shapes and sizes lined with dysplastic elongated hyperchromatic nuclei with frequent mitotic figures or stratified multilayered crowded nuclei with an extremely significant ($p<0.0001$) reduction of goblet cell number when compared to the control together with major pathological bone changes were observed in cc and the treated groups. While the protected group showed impressive improvement of all previously mentioned diameters.

**Key words: colon cancer rat, vitamin B17**

## INTRODUCTION

Colon cancer is often found in patients aged 50 years or older. However, recent interest in Egyptian colon cancer has been raised when epidemiological studies revealed a high incidence of this disease among young Egyptian population aged between 30-35 years [14]. The etiology of colon cancer is multifactorial, including genetic, environmental and dietary factors [2]. At diagnosis of colon cancer, 3.7-11% developed bone metastasis [12]. Animal models are good ways to study the disease development. In addition, these models allow for studying the prevention of colon cancer [7]. Currently experimental models use 1, 2-dimethylhydrazine (DMH) which is a potent colon carcinogen and the most widely used colon cancer inducer. DMH causes oxidative stress by methylating the molecules of colonic epithelial cells [5]. Colon cancer is considered to be a preventable disease [25].

Vitamin B17, commonly known as Laetrile or Amygdalin, is claimed to be a potential natural chemotherapeutic agent found particularly in the seeds of common fruits such as apricots, peaches and apples [9]. The anti-neoplastic effect of vitamin B17 is attributed to its ability to induce apoptosis in tumor cells. It is also claimed to reduce the mitotic activity of these cells [18]. It would be therefore worthwhile to experimentally induce a rat model of colon cancer and study the possible role of vitamin B17 whether protective or curative.

## MATERIALS AND METHODS

1, 2 Dimethylhydrazine dihydrochloride (DMH): A product of Sigma-Aldrich (Munich, Germany), was available in the form of white powder. It was dissolved in 1mM EDTA-Normal saline. It was given to the rat by intra-peritoneal injection (I.P) at a dose of 20 mg/kg/body weight once weekly for five consecutive weeks [23].

Vitamin B17: it was obtained online from (IHerb, California) in the form of capsules. The container served 100 capsules, each capsule served 100 mg Apricot seed extract (Vitamin B17) (Amygdalin). It was given at a dose of 300 mg/kg bodyweight daily by oral tube [24].

Eighty young adult male albino rats, weighing between 160-180 gm. were obtained from Theodor Bilharz institute's animal house, El-Warraq, Giza, Egypt. They were fed standard diet.

Ethical approval was obtained from the animal house of Theodor Bilharz Institute. Animals were divided into five main groups:

- Group I (Control Group): This group consisted of 10 male albino rats; they were subdivided into Subgroup Ia: consisted of 5 rats; they were kept without any treatment until the end of the study. Subgroup Ib: consisted of 5 rats, they received 1mM EDTA intra-peritoneal once weekly until the end of the study.
- Group II (Vitamin B17 group): consisted of 10 rats, they received the calculated dose of vitamin B17 orally daily for five weeks.
- Group III (colon cancer (CC) induced group): consisted of 20 rats, received the calculated dose of DMH I.P once weekly for five weeks.
- Group IV (Protected group): consisted of 20 rats; received first the calculated dose of vitamin B17 orally daily for 5 weeks then colon cancer was induced for the following 5 weeks.
- Group V (Treated Group): consisted of 20 rats; colon cancer was induced first with DMH injection by the dose mentioned above for 5 weeks, and then received the calculated dose of vitamin B17 for 5 consecutive weeks.

All rats were then sacrificed after 10 weeks.

**Clinical assessment**

Initial and final weights were recorded [11], blood samples were taken for assessment of CEA levels [12].

**Light microscopic study**

A small piece of the distal colon and lumbar vertebrae (cleaned of all soft tissue) were fixed for 24 hours in 10% neutral buffered formalin then dehydrated in ascending grades of alcohol, cleared and embedded in paraffin. After deparaffinizing, the 3-5 microns thick tissue sections were cut by microtome and were subjected to: Hx&E staining for routine histological examination, masson trichome staining (for colon sections) for detection of collagen fiber deposition, toluidine

blue (for bone sections) for assessment of bone mineralization and immunohistochemical stains for colon sections (ki-67 (marker of proliferation and detecting the mitotic activity), Cytokeratin 20 (CK20 for detecting adenocarcinoma arising from epithelia that normally contain this protein), vascular endothelial growth factor (VEGF for detecting angiogenesis), and Caudal Type Homeobox 2 (CDx2 protein involved in the proliferation and differentiation of intestinal epithelial cells via regulation of intestine-specific gene transcription with a tumor suppressor role).

**Scanning electron microscopic study** [14]

Samples from distal colon were subjected to post-fixation in 2% osmium tetroxide for two hours. They were then washed in distilled water for five minutes and passed through a series of graded acetones to achieve dehydration. Critical point drying was carried out with liquid carbon dioxide. The specimens were mounted on aluminum slabs using silver conductive paint and gold palladium sputter coating was achieved using a Polaron E5100 sputter coating instrument. The biopsies were examined by a scanning electron microscope (JEOL JSM35) at an acceleration voltage of 20 kV at EM unit at Faculty of medicine, Tanta University.

**Morphometric study**

H&E stain (colon sections): Goblet cells number & Mitotic index, H&E stain (bone sections): number of bone resorption pits, masson trichome stain: percentage of surface area of collagen fiber deposition, toluidine blue stain: color intensity & immune-stains: percentage of ki-67 immuno-positive nuclei, percentage of Ck20 immuno-positive nuclei, area percentage of VEGF & percentage of surface area of CDX2 positive immune-staining in all groups By using image analyzer software (Image J analyzer version 1.43o8, National Institutes of Health, USA and Digimizer version 4.3.5, MedCalc software). This was done in Anatomy and Embryology Department, Menoufia University.

**Statistical analysis** [15]

Statistical Analysis was performed for the initial and final weights, CEA and for the morphometric results. Results were collected, tabulated and statistically analyzed by statistical package for social science (SPSS) version 20 on IBM compatible computer. Results were expressed as mean ($\bar{X}$) ± standard deviation (SD). Student t-test (a test for significance comparing two groups) was performed. A value of $p < 0.05$ was considered significant. 10 rats were used for each.

## RESULTS

### General results

Both CC induced group and the treated group showed decreased physical activity when compared to the control group. 20 and 30% mortality was recorded for the CC induced group and the treated group respectively.

### Body weight

**Histogram 1** shows the body weight changes among the studied groups. Both CC induced group and the treated group showed significant ($p < 0.001$) decrease in their final body weight when compared to their initial ones. The protected group showed a non-significant decrease ($p > 0.05$) in their final weight when compared to their initial one.

### Biochemical results

**Histogram 2** shows the carcino-embryonic antigen (CEA) level among the studied groups. Compared to the control group, animals of the CC induced group showed a statistically significant increase ($p <0.001$) in their CEA level. The protected group showed a non-significant increase ($p > 0.05$) in its level. The treated one showed a significant increase ($p < 0.001$) in the serum CEA concentration.

### Histological results

All sections of both control and vitamin B17 groups showed nearly similar histological features with no statistically significant differences between them.

**Light microscopic study**

**H&E stain**

**Colon sections:** The colonic tissue of control group consisted of: the innermost layer is the mucosa, underneath this is the submucosa, followed by the muscularis propria and finally, the outermost layer - the adventitia. The structure of these layers varies, in different regions of the digestive system, depending on their function. The mucosa showed parallel straight crypts (colonic glands or acini) extending to the muscularis mucosa and separated by the lamina propria. The lining epithelium was composed of principle simple columnar epithelial cells with oval vesicular nuclei and mucous secreting goblet flask shaped cells with basal dense nuclei. CC induced group (Group III) showed disrupted mucosal continuity with abnormal sloughing and extrusion of the necrotic debris into the colonic lumen, invasion of the colonic tissue by pleomorphic branching colonic glands of variable shapes and sizes. The abnormal glands were lined with dysplastic elongated hyperchromatic nuclei with an extremely significant ($p < 0.0001$) increase in the number of mitotic figures or stratified multilayered crowded nuclei with an extremely significant ($p < 0.0001$) reduction of goblet cell number when compared to the control. Group IV showed preservation of the normal colonic architecture of the mucosa which appeared with preserved continuity. Most of the lining epithelial cells appeared with oval vesicular euchromatic nuclei; however, few lining epithelial cells showed mild to moderate dysplasia with elongated hyperchromatic nuclei. Some disruption of the muscularis mucosa with congested blood vessels in the sub-mucosa was evident. This group showed an extremely significant ($p < 0.0001$) decrease in the mitotic index and an extremely significant increase ($p < 0.0001$) in the goblet cell percentage when compared to the cc group. Group V showed more or less distorted colonic architecture with extensive sloughing of the abnormal mucosa into the lumen. The lining epithelial cells showed elongated hyperchromatic nuclei and a non-significant decrease in number of mitotic figures when compared to cc group. An extremely significant ($p < 0.0001$) reduction of goblet cell number was clearly evident. The muscularis mucosa layer was disrupted and the submucosa showed congested dilated blood vessel (Fig. 1, 2, Histogram 3, 4).

**Lumbar vertebra sections:** The bone tissue control group showed regular well-organized parallel arrangement of the bone lamellae. The osteocytes within the bone matrix were resident

inside their lacunae. The bone marrow space was filled of hematopoietic cells and scattered adipocytes. CC induced group showed an extremely significant increase ($p < 0.0001$) in bone resorption pits in the vicinity of multi-nucleated osteoclasts. The osteocytes appeared with wide lacunae. The bone lamellae lost their parallel well-organized arrangement with areas of sub-periosteal bone necrosis. The bone marrow spaces were widened and invaded by tumor cell nests with signet ring cells. The protected group revealed more or less preserved parallel arrangement of bone lamellae with an extremely significant decrease ($p < 0.0001$) in number of bone resorption pits compared to the cc group, together with presence of several multi-nucleated osteoclasts. The treated group showed tumor cell nests invading the bone marrow space and surrounding the destructed trabecular bone that showed a non-significant decrease ($p > 0.05$) of bone resorption pits number compared to cc group, with multi-nucleated osteoclasts (Fig. 3, Histogram 5).

**Special stains**

**Masson Trichome stain:** Comparing with the control group, cc induced group showed an extremely significant increase ($p < 0.0001$) in the surface area percentage of collagen fiber deposition. The protected group showed an extremely significant decrease ($p < 0.0001$) in the same percentage when compared to the cc group. When compared to the cc group, the treated group showed no statistically significant difference ($p > 0.05$) of the same percentage. When compared to the protected group, the treated group showed an extremely significant increase ($p < 0.0001$) in this percentage (Fig. 4).

**Toluidine Blue stain:** Comparing with the control group, CC group showed an extremely significant decrease ($p < 0.0001$) in the toluidine blue color intensity. The Protected group showed a very significant increase ($p < 0.001$) in the same percentage when compared to the colon cancer induced group. The treated group showed a non-significant decrease ($p > 0.05$) in toluidine blue color intensity when compared to the cc group, while showed an extremely significant decrease ($p < 0.0001$) in toluidine blue color intensity when compared to the protected group (Fig. 5).

**Immuno-stains:** Control group showed negative immune-staining for Ki-67, VEGF, mild positive immune-staining for Ck20 and marked positive immune-staining for CDx2. CC group showed strong positive immune-staining for Ki-67, VEGF and Ck20, while showed negative immune-staining for CDx2. The protected group showed mild to moderate positive reactions for all

immune-stains. The treated group showed marked positive immune-reaction for Ki-67, VEGF & Ck20, while showed negative reaction to CDx2 (Fig. 6, Histogram 6).

**Scanning Electron microscopic study:**

The control group revealed that the colonic surface mucosa was composed of rounded to oval well-arranged cryptal units. Each unit was covered with concentrically arranged epithelial cells with a central rounded lumen. The crypts were well-delineated by furrows. The cryptal units were loaded with mucous secretion. The cc group showed total loss of the epithelial cells covering the crypts. Moreover, necrotic areas of the surface mucosa were clearly evident. The surface mucosa was depleted of mucous secretion. The protected group showed more or less normal crypt units bathed with mucous secretion with preserved both covering epithelium and central lumen. However, some sections showed few abnormal crypts which lost their covering epithelium. The cryptal units of the treated group showed loss of their covering epithelium, others showed obliteration of the central lumen. Necrotic areas of the surface mucosa were clearly evident (Fig. 7).

**DISCUSSION**

With the increasing incidence of colon cancer worldwide with its very high morbidity and mortality rates and poor prognosis, several attempts were done to convert it to a preventable disease [11][5]. Vitamin B17 (Amygdalin), as a natural substance, may have anti-inflammatory and anti-cancerous effects. The role of Vitamin B17 in treating colon cancer is still a matter of controversy. In this study, the elevated serum CEA levels of the colon cancer induced group judged the occurrence of colon cancer which was further supported by the highly significant reduction in the final body weight of this group when compared to the initial one. Furthermore, colon cancer was evidenced by the major pathological lesions affecting the colon; this was in accordance with Moharib et al [15]. In the current work, the earliest hallmark for colon cancer was the presence of hyperplastic aberrant crypt foci which are abnormal crypts diverging from the normal shape. This was in agreement with Youssef et al. [28]. Hyperplasia of the crypts was further evidenced in this study by the scanning electron microscopic results that showed hyperplastic elevated crypts' epithelial covering. This was supported by Paulsen et al. [20]. Sanganna and Kulkarni, [21] stated

that hyperplasia might be due to the oxidative stress involved in the process of tumor development. This mechanism might explain the highly significant increase in the mitotic index of this group when compared to control as shown in our results. Furthermore, in the present work, the colon cancer induced group showed intense positive immunoreaction for Ki-67 which might prove the enhanced proliferative activity. All degrees of dysplasia have been reached; mild, moderate and severe dysplasia with finally the anaplasia or the carcinoma stage. This was in agreement with Jucaa et al. [11] who used the same methodology for completion of experimental carcinogenesis by DMH. Colon cancer group in this study showed strong positive immune-reaction for Ck20; which emphasized reaching the adenocarcinoma stage; this was in accordance with Nabil et al. [16]. In the present study, colon cancer induced group showed a highly significant decrease in the number of Goblet cells or their complete absence. This was further evidenced by our SEM study which revealed absence of the mucous secretion in this group. In this study, colon cancer group showed a highly significant increase of the percentage of collagen fiber deposition. Fibrosis might suggest the presence of chronic inflammation, thus chronic exposure of fibroblasts to inflammatory mediators may drive their transition to activated myofibroblasts with consequent abnormal collagen production. Colon cancer induced group showed highly significant decrease in the percentage of CDX2 positively stained surface area; this was in agreement with Sangeetha and Nalini, [22]. In the current study, angiogenesis (formation of new capillaries from pre - existing blood vessels) as one of the most leading factors to develop bone metastasis has been proved as colon cancer group showed strong positive expression of VEGF. Lumbar spine was the site of choice to assess the possibility of bone metastasis. This was in accordance with Jimi et al., [10] who postulated that the lumbar spine, followed by the pelvis were the most common sites of bone metastasis in colon cancer (62.16%-55.40% respectively). Cassar et al., [3] attributed vertebral metastasis from colon cancer to a vertebral venous plexus named Baston's plexus which was considered to be the main source of spreading. In the present study, bone metastasis was evident due to presence of multiple osteolytic lesions and resorption pits. Increased activity of the osteoclasts revealed the presence of osteolytic type of bone metastasis. This was in accordance with Macedo et al. [13]. The presence of tumor cell nests inside the bone marrow cavity emphasized the metastasis. These results were in line with Vatandoust et al., [27] who reported that signet ring cell stage of colon cancer had a high rate of bone osteolytic metastasis. In the current work, when compared to the cc group, the protected group showed nearly normal physical activity, average food intake, a non-significant difference between their final body weight and their initial one. No deaths occurred among this

group, marvelous regenerative changes proved by the significant improvement in serum CEA level and the Impressive improvement of the disrupted histology that appeared very close to reach the normal appearance. On the contrary, the treated group did not show any impressive improvement compared with colon cancer induced and protected groups. The present study showed significant decrease in collagen fiber deposition of the protected group when compared to the treated one. This might suggest the anti-fibrotic action of vitamin B17. This could be explained as vitamin B17 caused regression of inflammation with subsequent regressed fibrosis. This was in accordance with Bottinger and Bitzer, [1] who reported that vitamin B17 might enhance serum butyrate concentration which caused suppression of pro-fibrotic cytokine transforming growth factor beta 1 (TGF-β1). Moreover, Guo et al. [8] studied the effect of amygdalin in suppressing kidney fibroblast proliferation and TGF-β1 secretion in the lymphocytes and thus was able to significantly postpone the process of renal interstitial fibrosis, which further proved the anti-fibrotic effect of amygdalin. Furthermore, they hypothesized that the mechanisms which might be involved include increasing the secretion of type I collagenase, inhibiting kidney fibroblast proliferation, accelerating apoptosis and suppressing type I collagen synthesis. In the present study, the protected group showed mild positive immunoreaction for Ki-67 which might prove the inhibition of proliferative activity. This finding was in agreement with Park et al., [19]. The mechanisms of vitamin B17 in defeating cancer cells were uncertain; however, Cassiem and De-Kock, [4] performed a very recent study on vitamin B17's anti-cancer role. Being selective for destructing cancer cells which lack rhodanese enzyme, vitamin B17 exerts its anti-oxidant action. Normal cells do have the rhodanese enzyme which neutralizes vitamin B17 converting it to a harmless compound; thiocyanate. Meanwhile, cancer cells lack rhodanese enzyme, so cyanide radical is liberated. Moreover, Song and Xu, [24] added that Amygdalin could significantly increase polyhydroxyalkanoates (PHA) that induced human peripheral blood T lymphocyte proliferation with secretion of IL-2 and IFN-γ, and then inhibiting the secretion of TGF-β1, therefore enhancing the immune function. In the current work, treatment of colon cancer with vitamin B17 did not either induce improvement or reversal of the pathological changes that occurred. This might be due to the progressive and irreversible uncontrolled progressive cancer cell division and bone metastasis. Ki-67, Ck20 and VEGF all showed intense positive immunostaining when compared to the control group.

## CONCLUSIONS

Our findings revealed that daily intake of vitamin B17 may play an important role as a chemo-preventive, anti-cancer, anti-inflammatory, anti-fibrotic and anti-oxidant agent. Furthermore; this study proved the uselessness of vitamin B17 in curing colon cancer.


## Acknowledgment

Acknowledgment to all members of Human Anatomy and Embryology Department Faculty of Medicine-Menoufia University.


## References


1- Böttinger, E.P. and Bitzer, M. (2002): TGF-beta signaling in renal disease. J Am Soc Nephrol. 13:2600–2610.
2- Carethers, J.M. (2018): Clinical and genetic factors to inform reducing colorectal cancer disparitites in African Americans. Front Oncol.; 8: 531.
3- Cassar, N.; Cresswell, A. and Moran, B. (2017): Oligometastatic colorectal cancer: is single-site bony colorectal metastasis a treatable condition. Int J Colorectal Dis 2017; 32: 1229–31.
4- Cassiem, W. & De Kock, M. (2019): The anti-proliferative effect of apricot and peach kernel extracts on human colon cancer cells in vitro. BMC Complementary and Alternative Medicine; 19: 32.
5- Chari, K.Y.; Polu, P.R. and Shenoy, R.R. (2018): An appraisal of pumpkin seed extract in 1, 2-dimethylhydrazine induced colon cancer in wistar rats. Journal of Toxicology; 18:1-12.
6- De-Muth, J.E. (2014): Presentation Models in Basic Statistics and Pharmaceutical Statistical Applications, 3rd edition. CRC press (4): 95-61.
7- De-souza, A.S. and Costa-casagrande, T.A (2018): Animal models for colorectal cancer. Arq Bras Cir Dig.; 31(2): e1369.
8- Guo,J.; Wu, W.; Sheng, M.;Yang, S. and Tan, J. (2013): Amygdalin inhibits renal fibrosis in chronic kidney disease. Mol Med Rep.; 7 (5):1453-1457.
9- Jaswal, V.; Palanivelu, J. and Ramalingam C. (2018): Effects of the Gut microbiota on Amygdalin and its use as an anti-cancer therapy: Substantial review on the key components involved in altering dose efficacy and toxicity. Biochem Biophys Rep.; 14: 125-132.
10- Jimi, S.; Yasui, T., Hotokezaka, M., et al. (2013): Clinical features and prognostic factors of bone metastases from colorectal cancer. Surg Today; 43:751–6.
11- Jucáa, M.J.; Bandeiraa, B.C.; Carvalho, D.S. and Leal, A.T. (2014): Comparative study of 1,2-dimethylhydrazine and azoxymethane on the induction of colorectal cancer in rats. Journal of Coloproctology; 34(3):167–173
12- Li, A.A.; Yuan, Z.C.; Jia-Ming, L.; Shan-Hu, H. and Zhi-Li, L. (2018): The risk factors for bone metastases in patients with colorectal cancer. Medicine; 97(40): e12694.
13- Macedo, F.; Ladeira, K.; Pinho, F.; Saraiva, N.; Bonito, N.; Pinto, L. and Goncalves, F. (2017): Bone Metastases: An Overview. Oncol Rev.; 11(1): 321.
14- Metwally, I.H.; Shetiwy, M.; Elalfy, A.F.; Abouzid, A.; Saleh, S.S and Hamdy, M. (2018): Epidemiology and survival of colon cancer among Egyptians: a retrospective study. J coloproctol (rio j); 38(1): 24-29.
15- Moharib, S.A.; Abd El Maksoud, N.; Ragab, H.M. and Shehata, M.M. (2014): Anticancer activities of mushroom polysaccharides on chemicallyinduced colorectal cancer in rats. Journal of Applied Pharmaceutical Science; 4 (07): 054-063.

**16-** Nabil, H.M.; Hassan, B.N.; Tohamy, A.A.; Waaer H.F. and Abdel Moneim, A.E (2016): Radioprotection of 1,2-dimethylhydrazineinitiated colon cancer in rats using low-dose g rays by modulating multidrug resistance-1, cytokeratin 20, and -catenin expression. Human and Experimental Toxicology; 35(3): 282–292.

**17-** Nasir, N.L.; Kamsani, N.E.; Mohtarrudin, N.; Othman, F.; Tohid, S.F. and Zakaria, Z.A. (2017): Anticarcinogenic activity of Muntingia calabura leaves methanol extract against the azoxymethane-induced colon cancer in rats involved modulation of the colonic antioxidant system partly by flavonoids. Pharmaceutical Biology; 55 (1): 2102-2109.

**18-** Nour, A.; Azar, B.; Rabata, A. and Manadili, A. (2016): The Effect of Amygdalin in the Treatment of Squamous Cell Carcinoma induced in the Buccal Pouch of Golden Syrian Hamster. Journal of Dental and Medical Sciences; 15(2): 75-79.

**19-** Park, H.J.; Yoon, S.H.; Han, L.S.; Zheng, L.T., et al. (2005): Amygdalin inhibits genes related to cell cycle in SNU-C4 human colon cancer cells. World J Gastroenterol. ; 11(33):5156–61.

**20-** Paulsen, J.E.; Ellen Namork., and Alexander, J. (2005): Scanning Electron Microscopy of Colonic Lesions in 1, 2-Dimethylhydrazine-treated Rats. Anticancer Research 25: 3883-3888.

**21-** Sanganna, B. and Kulkarni, A.R. (2013): Effect of citrus reticulata essential oil on aberrant crypt foci (acf) development in 1, 2-dimetylhydrazine induced colon carcinogenesis rats. International Journal of Pharmaceutical Applications; 4 (1): 29-37

**22-** Sangeetha, N. and Nalini, N. (2015): Silibinin modulates caudal-type homeobox transcription factor (CDX2), an intestine specific tumor suppressor to abrogate colon cancer in experimental rats. Human and Experimental Toxicology; 34(1):56–64

**23-** Shewatatek, G., Wajana, L.L. and Getinet, Y. (2017): Coffee arabica complies chemo-preventive activity against DMH induced colorectal cancer in experimental rat model. J Med Diagn Meth; 6:1-3

**24-** Song, Z. and Xu, X. (2014): Advanced research on anti-tumor effects of amygdalin. J Can Res Ther; 10: 3-7.

**25-** Usher-Smith, J.A.; Walter, F.M.; Emery, J.D.; Win, A.K. and Griffin, S.J. (2016): Risk prediction models for colorectal cancer: a systematic review. Cancer Prev Res (Phila); 9(1):13-26.

**26-** Van Herck, H.; Baumans, B,; Brandt, C.J.W.M; Boere, H.A.G.; Hesp, A.P.M.; Van Lith, H.A. & Beynen, A.C. (2015): Blood Sampling from the Retro-orbital Plexus, the Saphenous Vein and Tail Vein in Rats: Comparative Effects on Selected Behavioral and Blood Variables. Lab. Anim.; 35: 131-139.

**27-** Vatandoust, S.; Price, T. and Karapetis, C. (2015): Colorectal cancer: metastases to a single organ. World J Gastroenterol; 21: 11767–76.

**28-** Youssef, K.M.; Ezzo, A.M.; El-Sayed, M.I.; Hazzaa, A.A; EL-Medany, A.H. and Arafa, M. (2015): Chemopreventive effects of curcumin analogs in DMH-Induced colon cancer in albino rats model. Future Journal of Pharmaceutical Sciences; 1: 57-72.

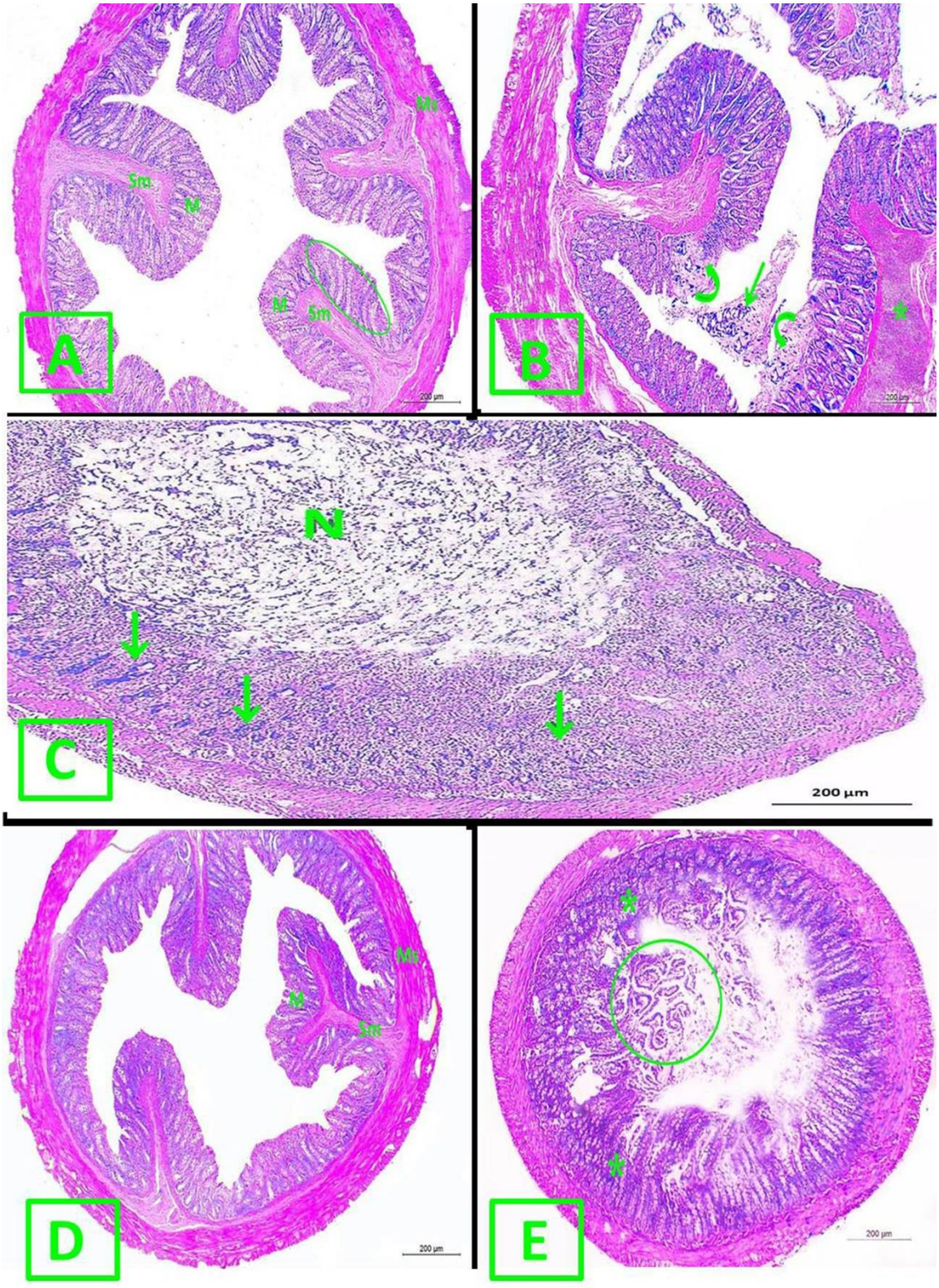


**Figure 1.** A photomicrograph of colon section in all experimental groups (H&E x40). **A.** Control group: Mucosa (M) with parallel colonic crypts (encircled), submucosa (Sm) and musculosa (Ms). **B, C.** CC induced group**:** disrupted mucosal continuity (curved arrows) with abnormal sloughed

tissue extruded into the lumen (thin arrow). C- Severely distorted colonic architecture with complete morphological loss of the mucosa and submucosa (arrows). Necrotic debris filling the colonic lumen (N)**. D.** Protected group: preservation of normal mucosal continuity (M). The submucosa (Sm) and musculosa (Ms) layers appear more or less normal. **E.** Treated group: more or less some distorted architecture. The mucosa and sub- mucosa are infiltrated by irregular crowded colonic glands (astrisks). Sloughing of the crypts into the colonic lumen (encircled)**.**

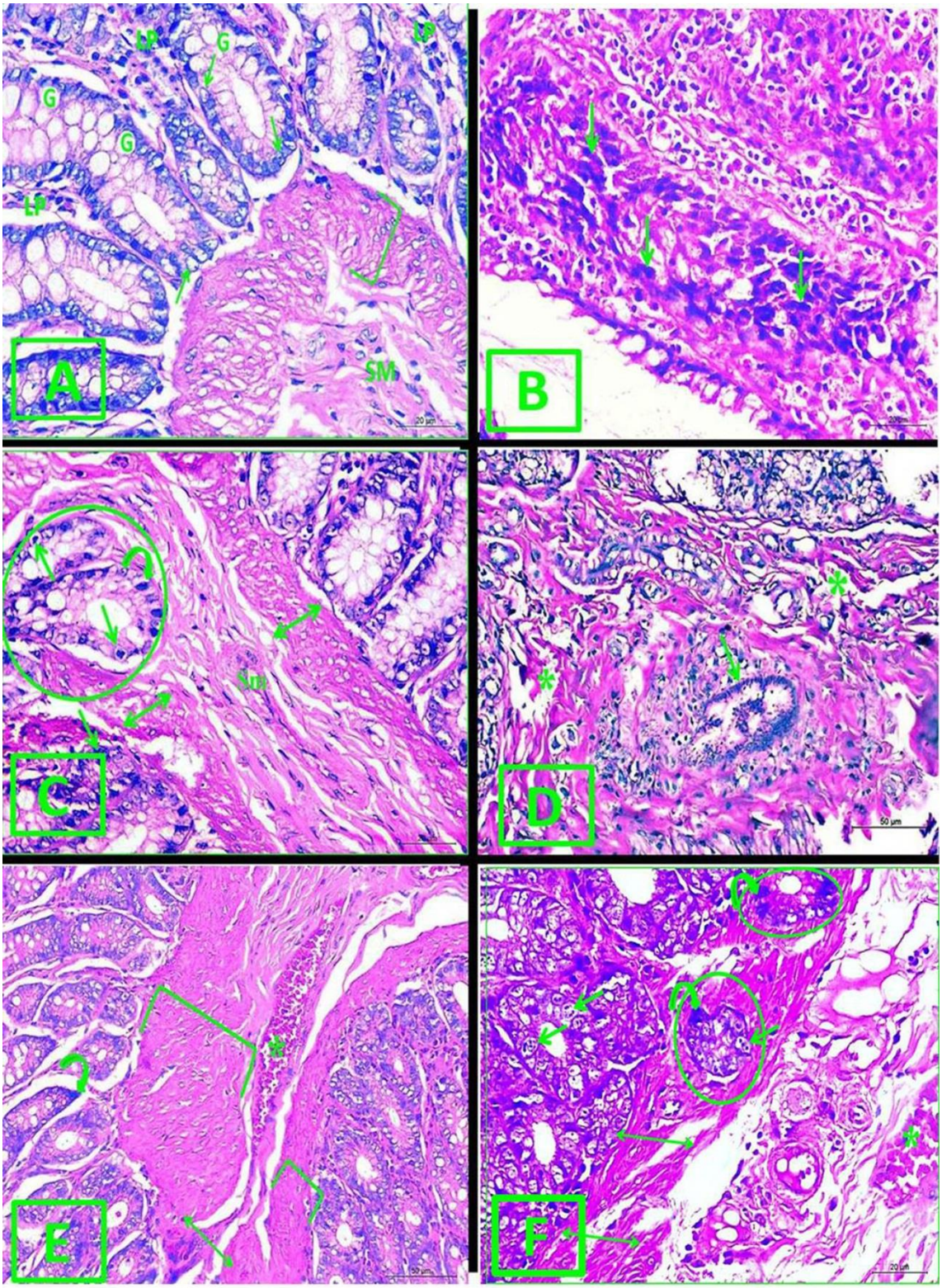


**Figure 2.** A photomicrograph of colon section in all groups (H&E x400). **A.** Control group: normal parallel colonic glands lined by simple columnar epithelial cells with oval vesicular nucleus (arrows) and mucous secreting goblet cells (G) with basal flat nuclei. Lamina propria (LP).

Muscularis mucosa (bracket). Submucosa (Sm). **B, C, D.** CC group: the atypical crypts lined with epithelial cells with elongated crowded hyperchromatic nuclei (arrows)**. C.** Atypical colonic glands (encircled) invading the muscularis mucosa layer (double headed arrows) reaching the submucosa (Sm). Some nuclei show frequent mitotic figures (thin arrow)**. D.** Abnormal pleomorphic colonic gland (thin arrow) lined with stratified multi-layered hyperchromatic crowded nuclei invading the musculosa layer (asterisks). **E.** Protected group: the majority of the crypts appear more or less normal. One abnormal shape crypt (curved arrow). Disrupted muscularis mucosa layer (double headed arrow). Asymmetrical appearance of muscularis mucosa (brackets). Congested dilated blood vessel in the submucosa (asterisk). **F.** Treated group: Abnormal glands (encircled) invading a disorganized muscularis mucosa layer (double headed arrow). The lining epithelial cells possess either elongated hyperchromatic nuclei (curved arrows) or frequent mitotic figures (thin arrows). Congested dilated blood vessel in the submucosa (asterisk)**.**

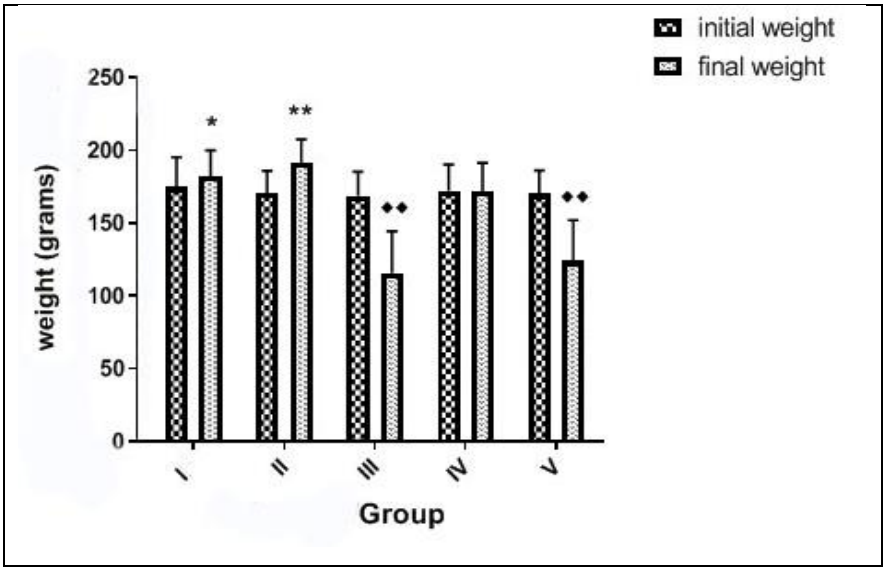


**Histogram 1.** Mean initial and final body weight of all rats (in grams): *, **Significant increase ($p < 0.05$ and $p < 0.001$, respectively) from the initial body weight; ♦♦Significant decrease ($p < 0.001$) from the initial body weight.

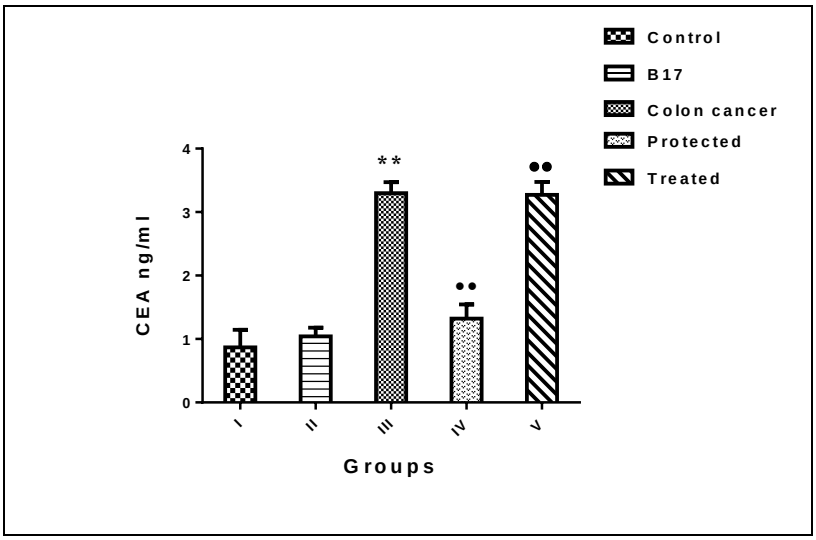


**Histogram 2.** Mean serum CEA concentration in all groups (ng/ml); **Significant increase from the control group ($p < 0.0001$). ••Significant decrease from the colon cancer induced group ($p < 0.0001$). ◦◦Significant increase from the protected group ($p < 0.0001$).

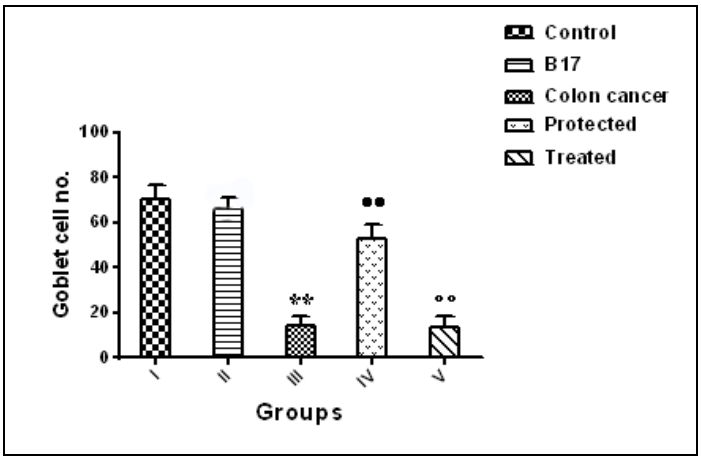


**Histogram 3. Mean Goblet cells percentage in all groups;** **Significant decrease from the control group ($p < 0.0001$). ••Significant increase from the colon cancer induced group ($p < 0.0001$). ◦◦ Significant decrease from the protected group ($p < 0.0001$).

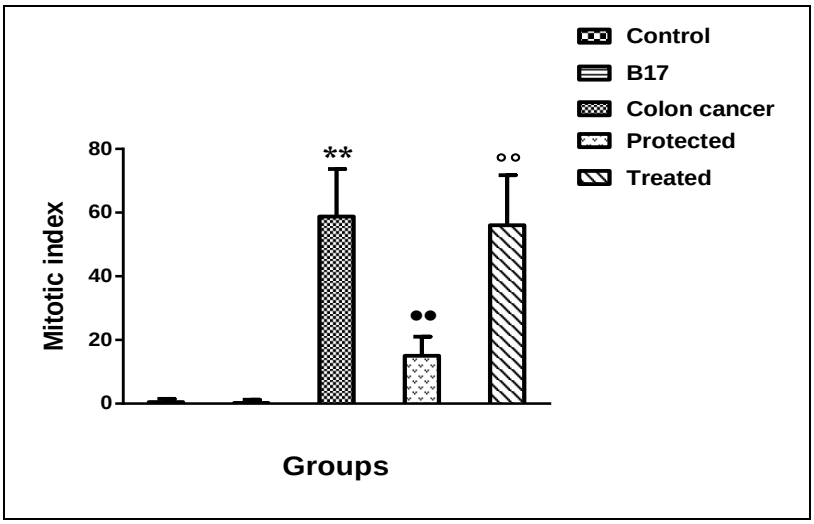


**Histogram 4. Mean mitotic index in all groups.** **Significant increase from the control group ($p < 0.0001$). •• Significant decrease from the colon cancer induced group ($p < 0.0001$). ◦◦Significant increase from the protected group ($p < 0.0001$).

Mitotic index = $\frac{\text{Number of mitotic figures} \times 100}{\text{Number of all evaluated cells}}$

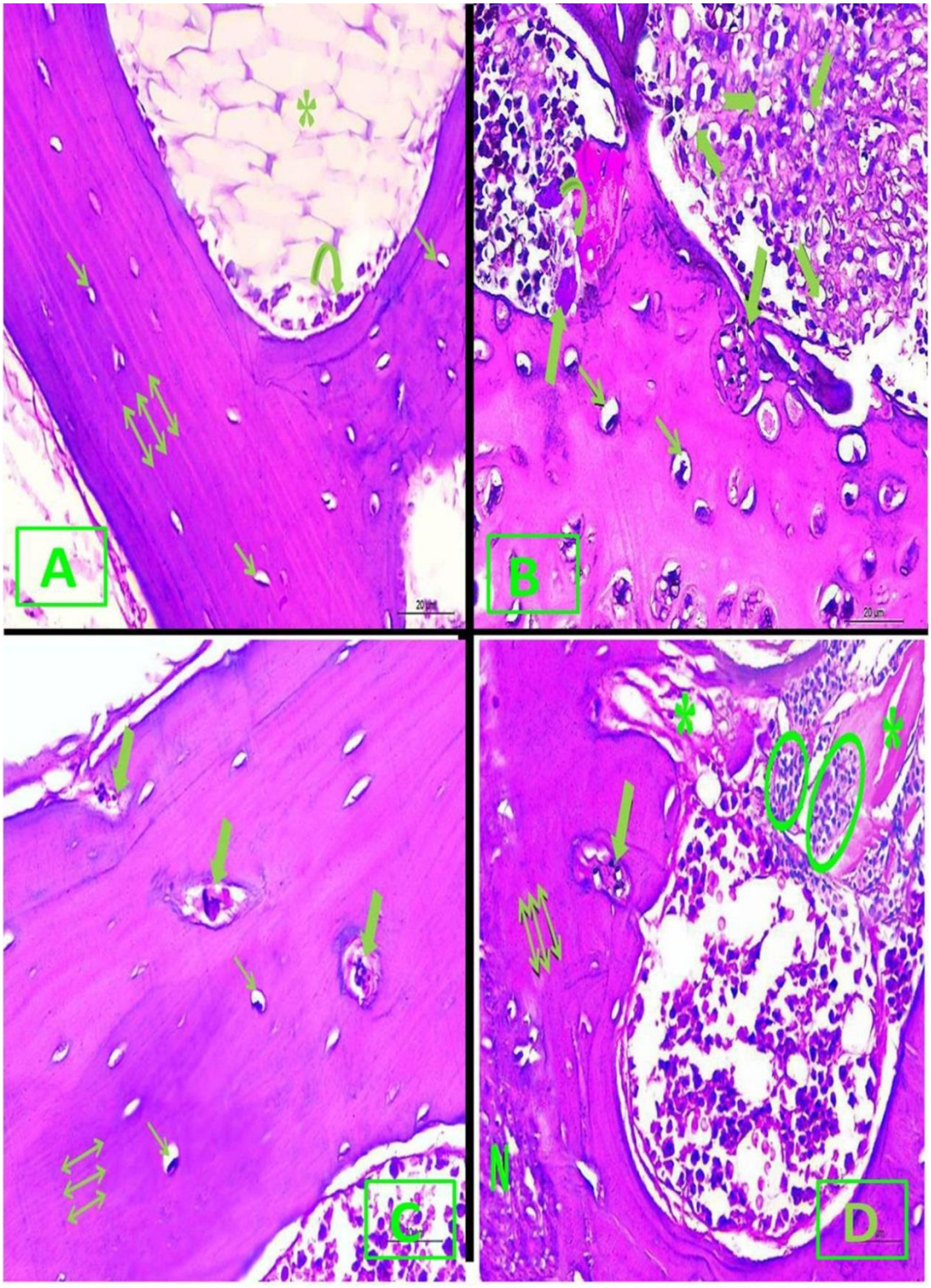


**Figure 3.** A photomicrograph of lumbar vertebrae section in all groups (H&E x400). **A.** Control group: regular well-organized parallel arrangement of the bone lamallea (double headed arrows). Osteocytes inside their lacunae (thin arrows). The bone marrow spaces can be seen with large

vacuolated adipocytes (asterisk) and heamopoitic cells (curved arrow). **B.** CC group: multinucleated osteoclasts (thick arrows) at the site of bone scalloping (curved arrow). Osteocytes with wide lacunae (thin arrows). Invasion of the bone marrow spaces by tumor cell nest with signet ring cells (notched arrows). **C.** Protected group: more or less preserved arrangement of the bone lamellae (double headed arrows). Multi-nucleated osteoclasts (thick arrows). Widening of the osteocytes' lacunae (thin arrows). **D.** Treated group: distorted arrangement of the bone lamellae (double headed arrows). Tumor cell nests (encircled) invading destructed bone trabaculea (asterisks). Multi-nucleated osteoclast (thick arrows). Area of bone necrosis (N).

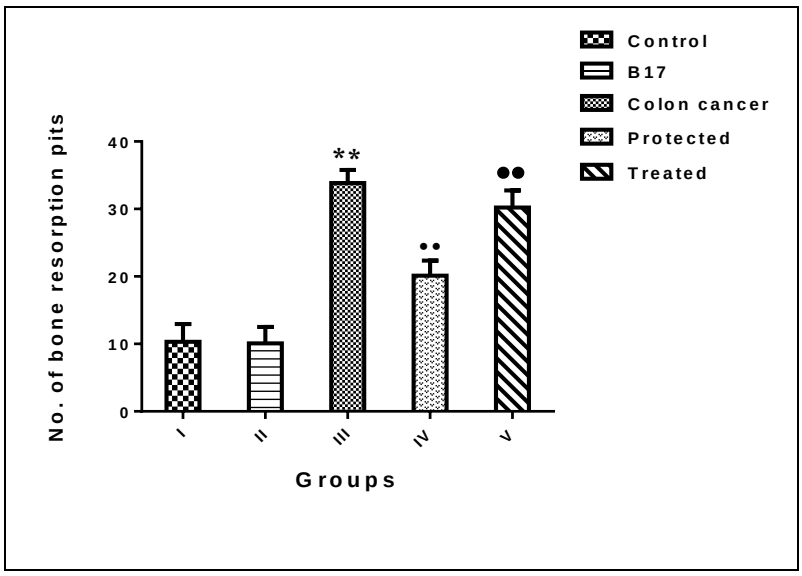


**Histogram 5.** Mean number of bone resorption pits; **Significant increase from the control group ($p < 0.0001$). ••Significant decrease from the colon cancer induced group ($p < 0.0001$). ◦◦Significant increase from the protected group ($p < 0.0001$).

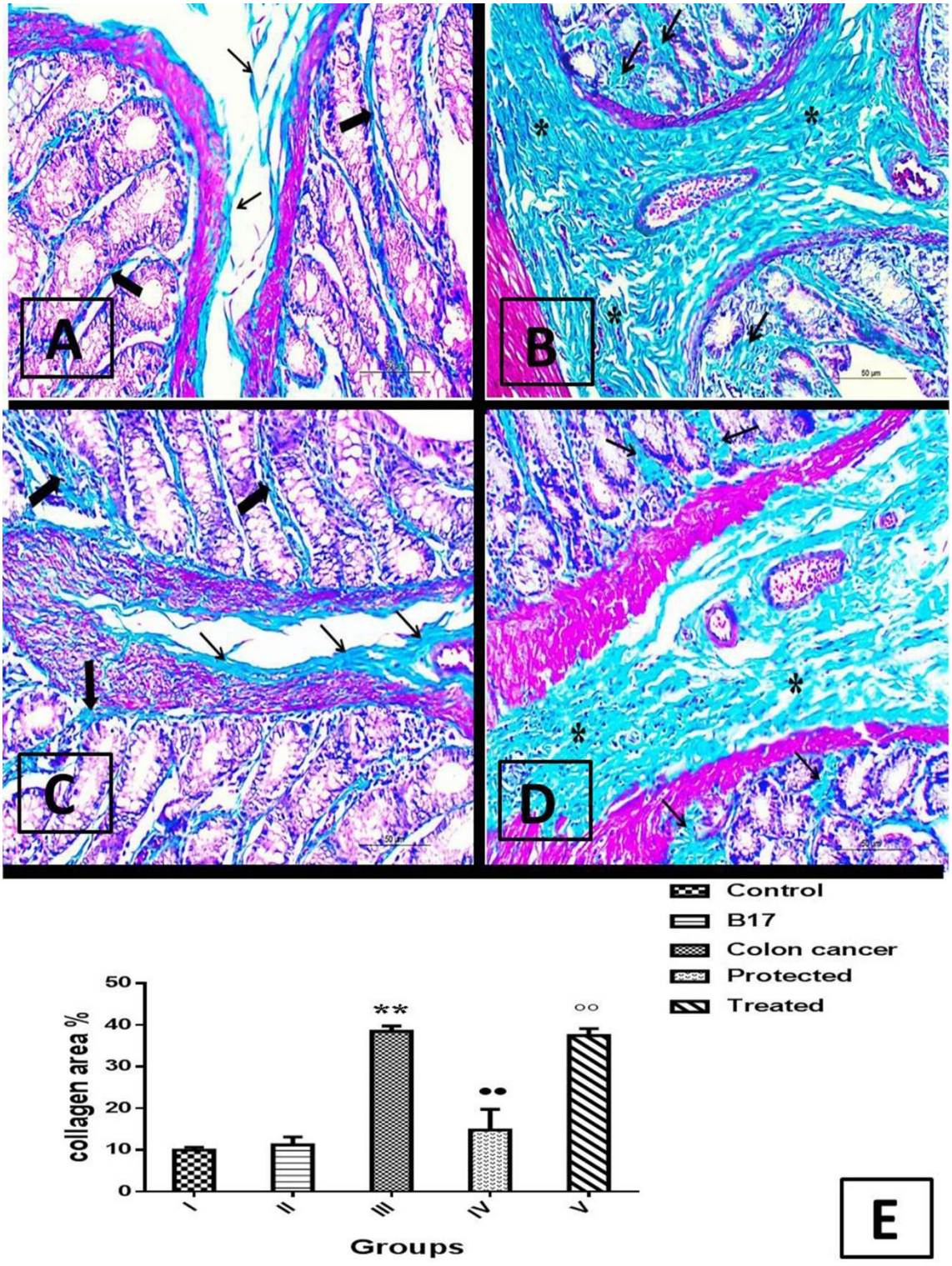


**Figure 4.** Photomicrographs of Masson Trichome stained colon sections of all groups (x400): **A.** Control group: minimal amount of collagen fiber deposition (arrows) **B.** CC induced group: large amount of collagen fiber deposition (arrows and asterisks). **C.** Protected group: small

amount of collagen deposition (thick and thin arrows). **D.** Treated group: large amount of collagen fiber deposition (arrows and asterisks). **E.** ** Significant increase from the control group ($p<0.0001$) •• Significant decrease from the cc group ($p<0.0001$). ◦◦Significant increase from the protected group ($p<0.0001$).

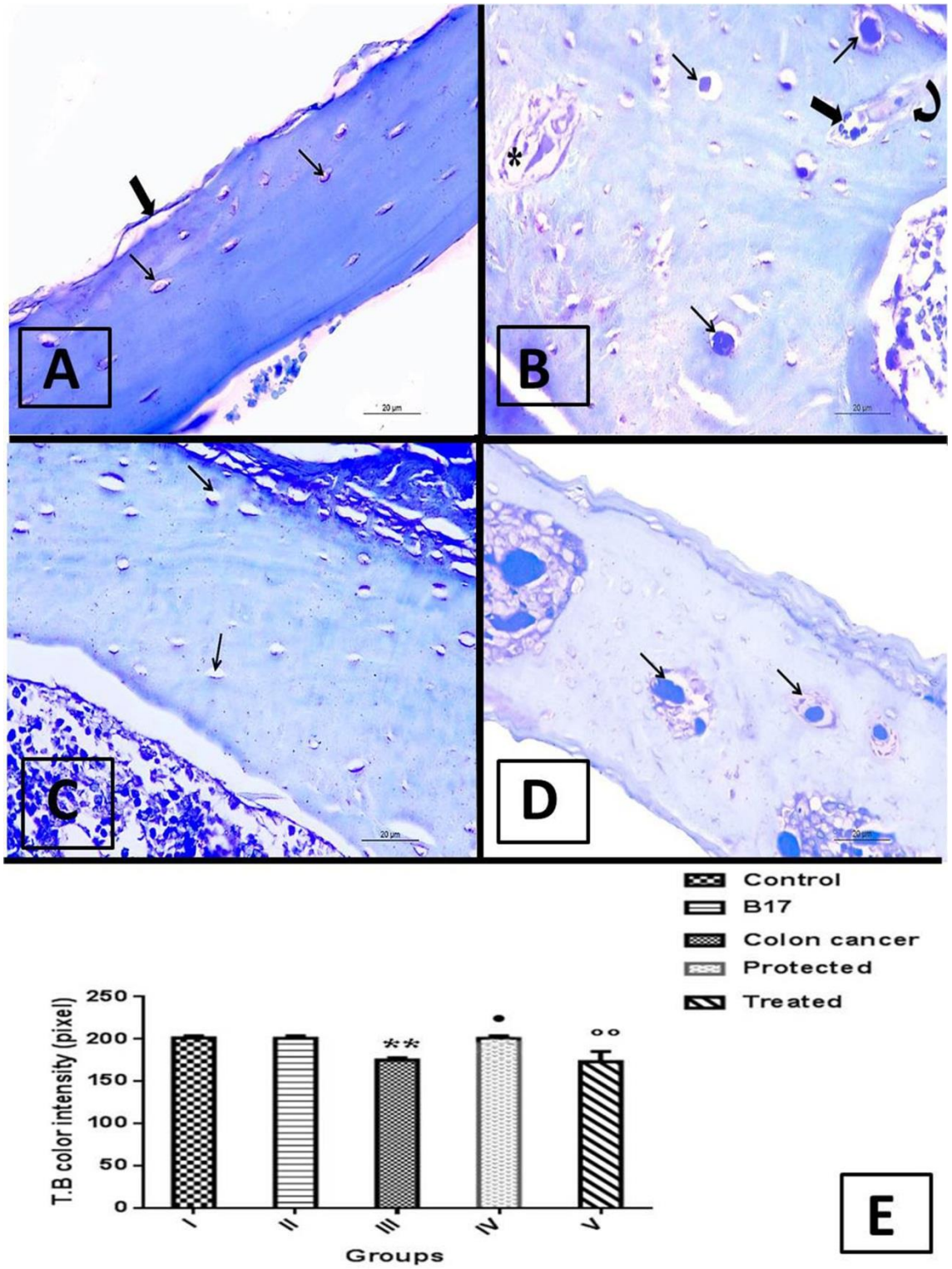


**Figure 5.** Photomicrographs of Toluidine Blue stained lumbar vertebral sections of all groups (x400). **A.** Control group: dark blue staining of the bone sections. **B.** CC group: faint blue staining of the bone sections. **C-** Protected group: Average blue staining of the bone sections. **D.** Treated

group: pale blue staining of the bone sections. **E.** Foote notes: ** Significant decrease from the control group ($p<0.0001$). •Significant increase from the colon cancer induced group ($p<0.05$). ◦◦ Significant decrease from the protected group ($p<0.0001$).

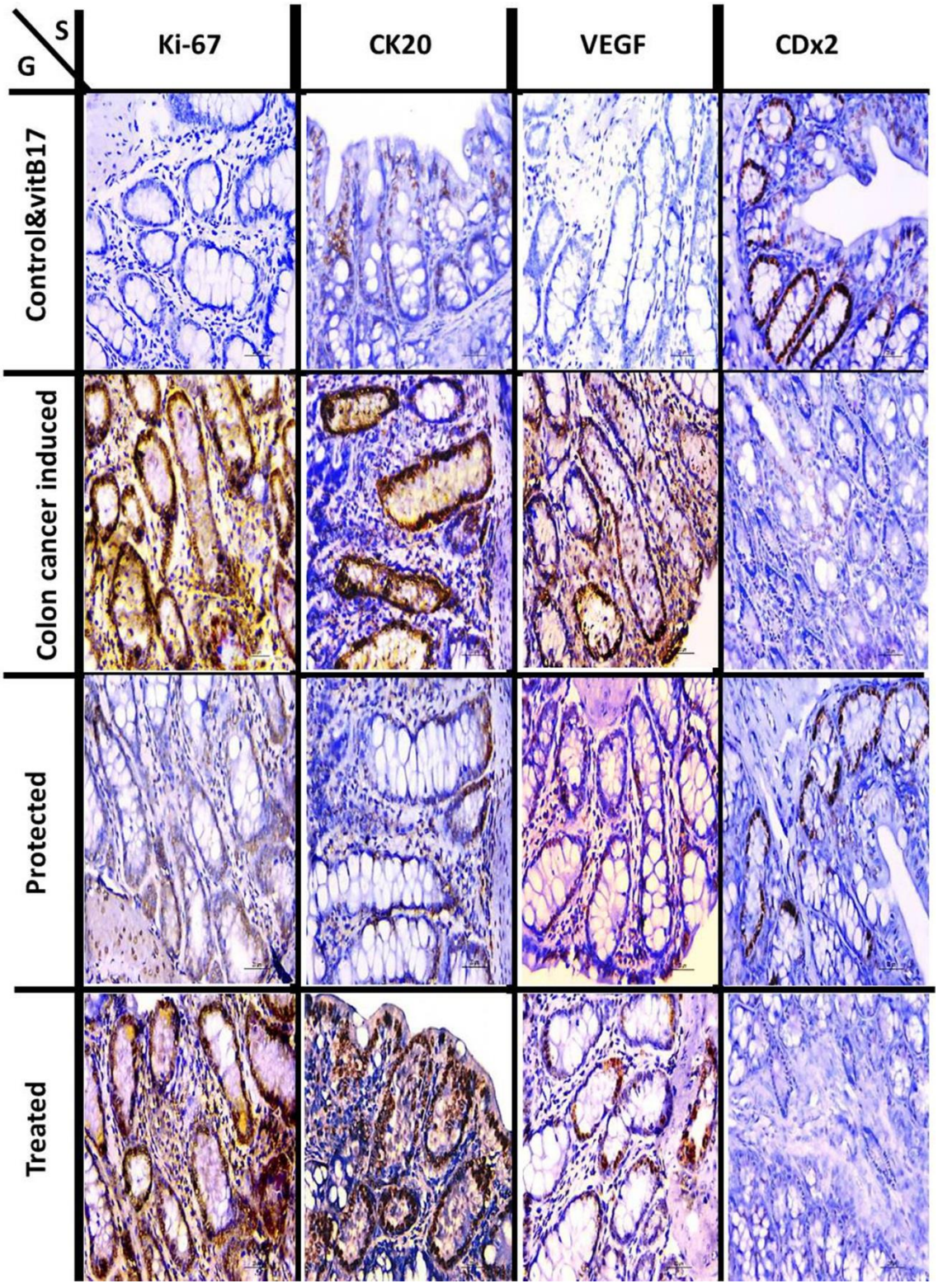


**Figure 6.** Photomicrographs of immuno-stained colon sections of all groups (x400): **Control & vitamin B17 groups:** negative immune-staining for Ki-67, Ck20, VEGF and positive for CDx2. **CC induced group:** strong positive immune-staining for Ki-67, Ck20, VEGF and negative for

CDx2**. Protected group:** mild to moderate immune-reaction for all immune-stains. **Treated group:** strong positive immune-staining for Ki-67, Ck20 and VEGF, but negative reaction to CDx2 immuno-stain; S — stain; G — group.

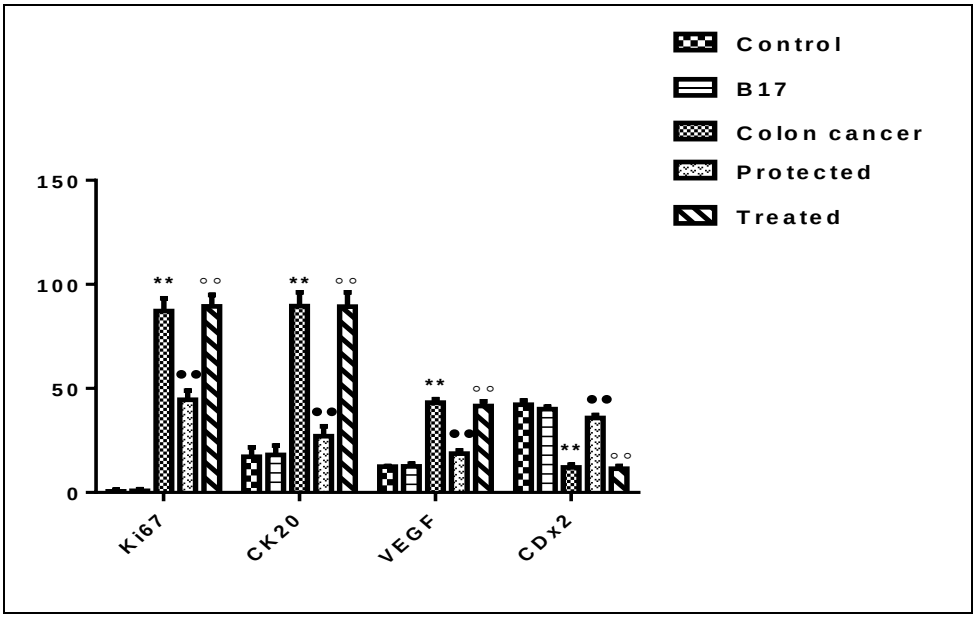


**Histogram 6.** Mean area percentage of immune-positive nuclei (%) in all groups: **Significant increase ($p < 0.0001$) from the control group (for Ki67, Ck20 and VEGF) and Significant decrease ($p < 0.0001$) from the control group for CDx2. ••Significant decrease from the cc group for ki67, ck20 and VEGF and significant increase from cc group for CDx2 ($p < 0.0001$). ◦◦Significant increase from the protected group for ki67, ck20 and VEGF and significant decrease from protected group for CDx2 ($p < 0.0001$).

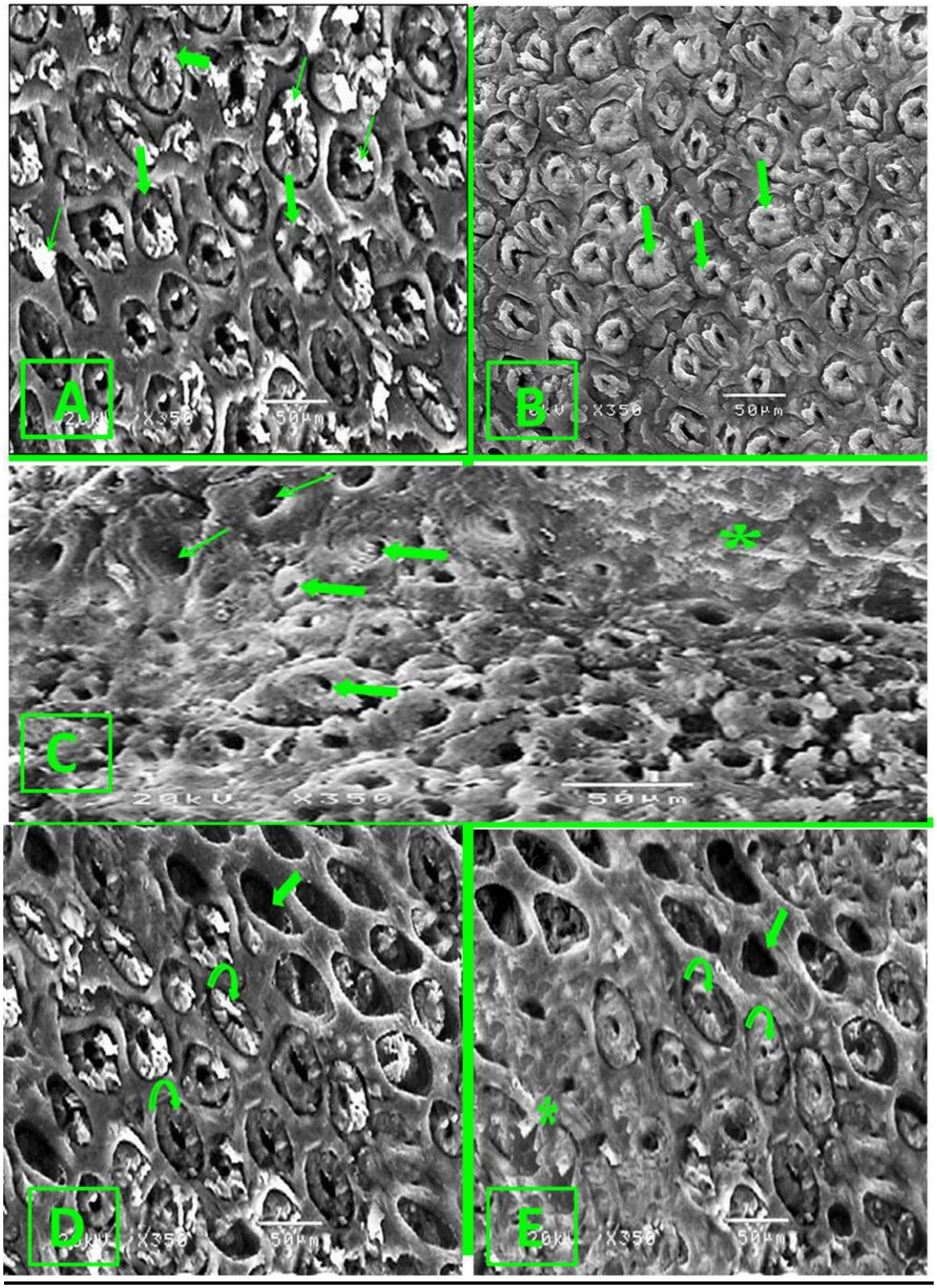


**Figure 7.** Scanning electronmicrographs of colon sections of all groups (SEMx 350): **A.** Control group: rounded to oval crypt units (encircled) covered with concentrically arranged epithelial cells, each unit is demarcated by a furrow (thick arrow) with a lumen at the center (asterisk). Mucous

secretion can be noticed (thin arrows). **B.** CC induced group: elevated crypt units with hyperplasia (arrows)**. C**. CC group: crypts with narrowed slit like lumen (thick arrows), others show wide crypt lumen with total loss of the cells covering the crypts (thin arrows). A necrotic area can be observed (asterisk). **D.** Protected group: some crypts appear more or less normal (curved arrows), others show complete loss of their covering cells (thick arrow). E- Treated group: crypts with obliterated lumen (curved arrows), others show total loss of their covering epithelium (thick arrow). A large necrotic area can be noticed (asterisk).